Optical Measurements of the Skin Surface to Infer Bilateral Distinctions in Myofascial Tissue Stiffness

Anika R. Kao, Zack T. Landsman, Gregory J. Gerling University of Virginia Charlottesville, USA Mary T. Loghmani Indiana University Indianapolis, USA

Abstract—About half the U.S. adult population suffers from chronic neuromusculoskeletal pain. While its evaluation and treatment are widely addressed by therapies using soft tissue manipulation (STM), their efficacy is based upon clinician judgment. Robust biomarkers are needed to quantify the effects of STM on patient outcomes. Among noninvasive methods to quantify the mechanics of myofascial tissue, most are limited to small (<10 mm²), localized regions of interest. In contrast, we develop an approach to optically simultaneously measure a larger (~100 cm²) field of deformation at the skin surface. Biomarkers based on skin lateral mobility are derived to infer distinctions in myofascial tissue stiffness. In specific, three cameras track ink speckles whose fields of deformation and stretch are resolved with digital image correlation. Their ability to differentiate bilateral distinctions of the cervicothoracic region is evaluated with four participants, as a licensed clinician performs STM. The results indicate that the optically derived surface biomarkers can differentiate bilateral differences in skin mobility, with trend directions within a participant similar to measurements with an instrumented force probe. These findings preliminarily suggest skin surface measurements are capable of inferring underlying myofascial tissue stiffness, although further confirmation will require a larger, more diverse group of participants.

Index Terms—Soft tissue manipulation, digital image correlation, massage, manual therapy, skin mechanics, touch, tactile.

I. INTRODUCTION

Chronic neuromusculoskeletal pain afflicts up to half of the adult population in the U.S. and is the most commonly reported health reason for receiving soft tissue manipulation (STM) or massage [1]–[5]. STM is a form of mechanotherapy that imparts mechanical forces through the intact surface of the body and can be delivered by hand contact alone or assisted with an instrument, such as a rigid sphere or flat blade [6]-[10]. Physical therapists use STM with approximately 85% of their patients [11]–[13]. When performing STM, the clinician simultaneously evaluates several tissue factors, including stiffness magnitude, area of greater stiffness, tissue mobility, and turgidity of inflammation. While the magnitude, angles, and timing of forces delivered to tissues, and responsive effects perceived from tissues, seek distinct clinical effects, STM practice mostly relies on subjective, nonspecific, and qualitative descriptors [14]–[18]. Progress to show the direct effects of soft tissue therapies on patient outcomes will require the development of quantitative biomarkers with robust signal-to-noise ratios among patients.

Numerous methods to quantify the mechanics of biological tissues, from ultrasound elastography to force-sensing devices,

have sought to characterize the viscoelastic properties of biological tissues. For instance, ultrasound-based methods displacement, shear wave differences, microvascular changes to perturbations in muscle and nerve tissue [19], [20]. Other imaging approaches, e.g., optical coherence tomography, capture small planes of data (a few mm) to estimate tissue layer thickness and relative density. Distinct from imaging, myotonometer devices use accelerometer recordings to assess the tension, elasticity, and stiffness of myofascial tissues, while load cells generate force-displacement curves from which stiffness is derived. While each method can estimate the mechanical properties of muscle and deep tissues, each is limited to localized regions of interest, usually spanning areas of less than 10 mm². As a consequence, to analyze larger muscles, which may span areas larger by an order of magnitude, these devices must be sequentially repositioned, which makes the analysis of viscoelastic properties challenging.

Observations of the skin surface could evaluate larger regions of interest, and thereby offer complementary insights into the mobility of underlying myofascial tissues. Large surface areas have been imaged using depth and general-purpose cameras from multiple angles [21]-[29]. From such data, distinct analysis approaches characterize surface movements. While disparity map techniques well capture 3D surfaces at distinct time points, they do not track the movements of individual pixels between time points, and as such cannot characterize stretch [28]. In contrast, approaches based upon digital image correlation track regions with distinct patterns of random pixels over time and therefore can evaluate surface stretch; and further, can stitch together multiple 3D surfaces to track large areas (tens of cm) and curvatures at high resolution, while avoiding occlusions [30]-[35]. While optical cameras cannot penetrate muscle, observations at the skin surface can provide indirect information about underlying tissue responses to surface indentation, pulling, and twisting forces.

In this work, we develop mechanical biomarkers based on surface observations of skin lateral mobility, and evaluate their ability to infer myofascial tissue differences against stiffness measurements of a load cell. The development of sensitive biomarkers that do not impede direct skin contact of clinicians may enable greater precision in assessing myofascial pain.

II. METHODS

This work uses a surface imaging approach to develop mechanical biomarkers, derived from skin lateral mobility, and evaluates their sensitivity in inferring bilateral distinctions in myofascial stiffness between a participant's left and right upper

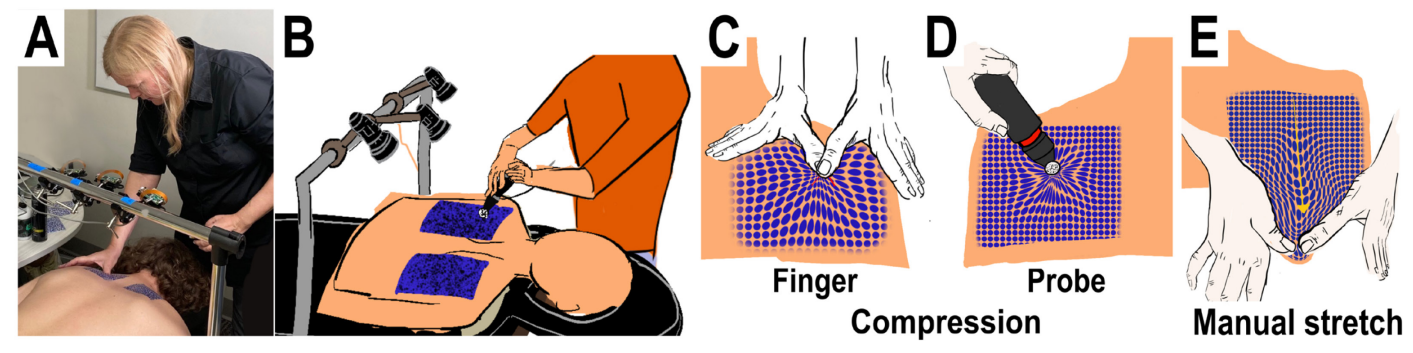


Fig. 1. Equipment setup, participant positioning, and manual manipulation procedures. (A) The clinician assesses the myofascial tissue mobility of the left cervicothoracic region of a participant. Participants assumed a standardized, prone position, with their arms at their sides (palms up) and feet resting on a bolster. An ink speckle pattern was applied to the left and right cervicothoracic regions for skin surface tracking with three overhead cameras. (B) An idealized abstraction of the experimental setup, with the three-camera setup, speckled skin regions, and instrumented force probe. The clinician applies compression to the left trapezius. (C) An abstraction of clinical administration of manual soft tissue compression with two hands, where the displaced speckles show inward movement toward the point of application. (D) Similar administration of compression using the instrumented force probe. (E) Administration of manual pull in the inferior direction, where the yellow arrow depicts the movement of speckles, and as such, skin displacement, in the direction of the pull.

back regions during soft tissue manipulation. To do so, new techniques and methods are developed, with experiments evaluating their utility performed by a clinician in the cervicothoracic region on four participants. In particular, using imaging from three cameras, an approach using digital image correlation captures the 1st principal stretch at the skin surface upon its manual clinical pull in four directions. Similar optical measurements are made as the clinician compresses the tissue normal to its surface with her fingertips and an instrumented force probe. From the recorded data, we explore a set of mechanical biomarkers built up from skin displacement and strain measurements, including skin stretch, direction and magnitude of applied pull, and depth and pattern of normal displacement. Ultimately, we chose a skin mobility biomarker that compares the minimum 1st principal stretch against the maximum applied pull. For comparative purposes, a baseline measure is acquired in other experiments using an instrumented force probe to capture a force-displacement tissue response. The two approaches are compared to determine the ability of the skin mobility biomarker to capture bilateral differences in myofascial stiffness per participant with similar relative trends, i.e., greater stiffness per side of the body.

A. Equipment setup and participant positioning

A portable massage table was set up whereby participants assumed a prone position to receive soft tissue manipulation (Fig. 1A-B). The face cradle was adjusted to ensure the neck was free of strain. An adjustable height aluminum bar was positioned above the massage table (~0.5 m) upon which were mounted, via ball socket clamps, three monocular cameras (12 MP, Raspberry Pi High Quality, UK) with wide angle lenses (6 mm Vilros, Lakewood, NJ, USA) connected to microcontrollers (Raspberry Pi Zero W boards, UK). The images from these cameras served as input into the image analysis pipeline.

B. Ink-based speckling method

In using digital image correlation (DIC), attaining displacement fields of high spatial resolution depends on the size and size consistency of the applied speckle pattern, the density and randomness of their pattern, and a high foreground-to-background contrast ratio with equal amounts of light and dark on the specimen surface. To meet these conditions and minimize

the impact on natural skin mechanics, an ink-based stencil transfer paper method was developed. A carbon thermal stencil machine (ATOMUS, China) was used to print a generated speckle pattern onto a 215.9 by 279.4 mm sheet of non-toxic, blue ink, hectograph paper. Prior to application, each participant's skin was cleaned with an alcohol wipe, and a nontoxic stencil application solution (Stencil Stuff, CA, USA) was lightly applied to the region of interest to ensure a clean transfer with minimal ink bleeding. After about 30-60 sec of drying time, the protective sheets were removed from the hectograph paper and the speckle pattern was pressed firmly onto the participant's skin surface and held for 30 sec to allow for proper absorption. The speckle sheet was then gently peeled off and the transferred speckle pattern was left to dry for 1-2 min. Once dry, a stencil setting spray (Stencil Stuff, CA, USA) was applied as a sealant for the speckle pattern, followed by a light coat of hair spray to reduce smudging when contacted by the clinician's hands. The pattern was then dried for another 5 min to ensure proper setting. Example results of this method are shown in Fig. 2A. After the experiments concluded, the ink was fully removed with a nontoxic alcohol wipe.

C. Imaging approach using 3D digital image correlation

DIC is a non-contact, optical tracking technique that matches pixel patterns from multiple stereo camera angles to produce displacement and strain fields [36], [37]. It allows for multiple 3D surfaces to be stitched together to avoid occlusions and thereby accommodate highly curved surfaces. DIC uses cross-correlation of the stereo-calibrated camera sets to measure movements of unique pixel patterns across frames. While one camera can track 2D images, a calibrated pair of cameras can correlate 2D information to produce 3D representations. Moreover, surfaces from multiple camera pairs can be merged into a cohesive surface of maximum correlation. A stereo camera calibration step is completed before data collection, to determine each camera's field of view and ensure overlap.

We used open-source software MultiDIC [36], built atop Ncorr [37], to capture 3D skin surface displacements, strain and stretch fields, etc. Video from each of the three cameras was captured synchronously by parallel computing at 30 frames per sec in 1920 by 1080-pixel resolution (~5 pixels/mm) and compressed into H.264 video format. As each experiment lasted

15 to 90 sec, after videos were converted back to images (450 - 2,700 images), data were down-sampled to 3 frames per sec to reduce excessive processing time. Raw images in grayscale were input into the DIC software for computation. Based on the diameter of ink speckles on the skin and the nature of STM surface deformation, the subset radius was set to 25 pixels and spacing to 5 pixels to optimize feature tracking and data resolution.

D. Instrumented force probe

An instrumented device was developed to measure the force and displacement of a rigid sphere upon its manual indentation into the skin and myofascial tissue of a human participant. A rigid sphere tip (19 mm) made of solid plastic was mounted to a multi-axis load cell (Nano17, ATI Industrial Automation, Apex, NC) and connected to a handle, within which an electromagnetic tracker (Flock of Birds, Ascension trakSTAR / driveBAY) was embedded. The load cell measures force in six directions. For this study, we used force in the normal direction (F_z) , where we can achieve 1/320 N resolution and 30 N range, at a 300 Hz sampling rate. Displacement can be monitored in six directions, as well, at 1.4 mm RMS resolution and 1.5 m range, and sampled at 300 Hz. For this work however, due to the higher inherent accuracy of the DIC method, we generated displacement measurements from observations of the sphere tip in the image frames.

III. EXPERIMENTS

A. Overview of soft tissue manipulation

In deploying specific STM techniques, a clinician assesses tissue for tenderness, induration (hardness), restrictions, and mobility in multiple directions. In our experiments, two types of STM, manual compression and manual pull, were performed to evaluate the myofascial tissue of the cervicothoracic region (Fig. 1C-E). First, tissue compression was performed manually by direct contact with the clinician's fingers, then with the instrumented force probe. Second, the manual pull of tissue was performed by the clinician's fingers in four lateral directions.

1) Manual and instrumented force probe compression: With either method, static force was applied perpendicular to the myofascial plane of the body surface, at a 5 sec rate to maximum force, as judged clinically. While using this technique, the clinician assesses the depth of penetration (deformation of tissue layers), area in contact with fingers or sphere tip, stiffness, deformation, modulus, and structures affected at various forces. Measurements of imposed displacement, applied force, and skin surface deformation were taken simultaneously.

2)Manual pull: Static force was manually applied in a direction horizontal to the myofascial plane, at a steady ramp-up rate of about 5 sec to a maximum force, with a 45-degree angle used to assess fascial mobility. Force was applied in four lateral directions (superior towards neck, inferior away from neck, medial towards midline, lateral away from midline) from a central focal point (e.g., tender spot) [19], [38]. Clinically relevant assessment factors include the spatial distance and velocity of force propagation from the point of application, the point of force magnitude and deformation at which discomfort (if any) is reached, the magnitude of force required to reach

maximum myofascial stretch, and any identified restrictions or barriers to fascial motion. Skin surface measurements were made of displacement magnitude and direction, with and without rigid body motion, or motion in which the distance between any two internal points remains unchanged, 1st principal Lagrangian strain, 1st principal stretch, normal indentation depth, and 2D cross-sectional curvature.

B. Experimental procedures and participants

A total of 14 experiments were conducted per participant, at a duration of 2 hours per participant. The 14 experiments consisted of 4 manual compressions (left and right, trials 1 and 2), 4 instrumented force probe compressions (left and right, trials 1 and 2), 4 manual pulls (left and right, trials 1 and 2), and a brief soft tissue treatment via 2 static holds, described in depth below. Participants followed an intake procedure given by the clinician (20 min). Following intake, participants were positioned in a standardized, prone position, with their arms at their sides (palms up) and feet resting on a bolster. The cervicothoracic junction (C7/T1), superior medial border of the scapulae, and distal insertion of the levator scapulae were palpated and marked with a black dot, bilaterally (5 min). Each bilateral region was then speckled following the procedure in II.B. (15 min). In trial 1, a standard procedure was used for manual STM assessment, first on the left side of the body, then on the right. In specific, manual compression was performed first, instrumented force probe compression next, and then manual pull in four directions. At the completion of trial 1, a brief soft tissue treatment was given via manual compression held statically near the most tender spot, per bilateral side, for one min. In trial 2, the procedure from trial 1 was repeated.

Four healthy individuals (1 male, 3 female, 26.5 ± 0.6 years of age, mean \pm SD) participated. All participants reported being right-hand dominant, fit the inclusion criteria of reporting moderate tension in the upper back, and provided written informed consent, as approved by the local institutional review board. Surfaces were sanitized following COVID-19 protocols.

IV. RESULTS

As indicated in Fig. 2, upon the clinical application of manual pull of skin in the medial and superior directions, data for one participant show the change in displacement, including rigid body motion (Fig. 2C, F), as well as the 1st principal Lagrangian strain (Fig. 2D, G) at the time point of maximum manual pull. In Fig. 2C, for example, the greatest displacement (about 25 mm) is in the direction of the manual pull, nearest the point of contact of the clinician's finger. Moreover, the directional movement of the skin is distinct between manual pulls in medial and superior directions, in Figs. 2C and F, respectively. Next, we describe the skin mobility biomarker, to be compared bilaterally, and against measurements of tissue stiffness obtained using the instrumented force probe.

A. Skin mobility biomarker

To assess skin mobility, we developed a biomarker representing the relationship between the minimum 1st principal stretch and maximum manual pull, per anatomical direction (Fig. 3). This is described in three steps. First, to determine the direction of the manual pull, the displacement of the entire speckled region of the skin surface is separated into four

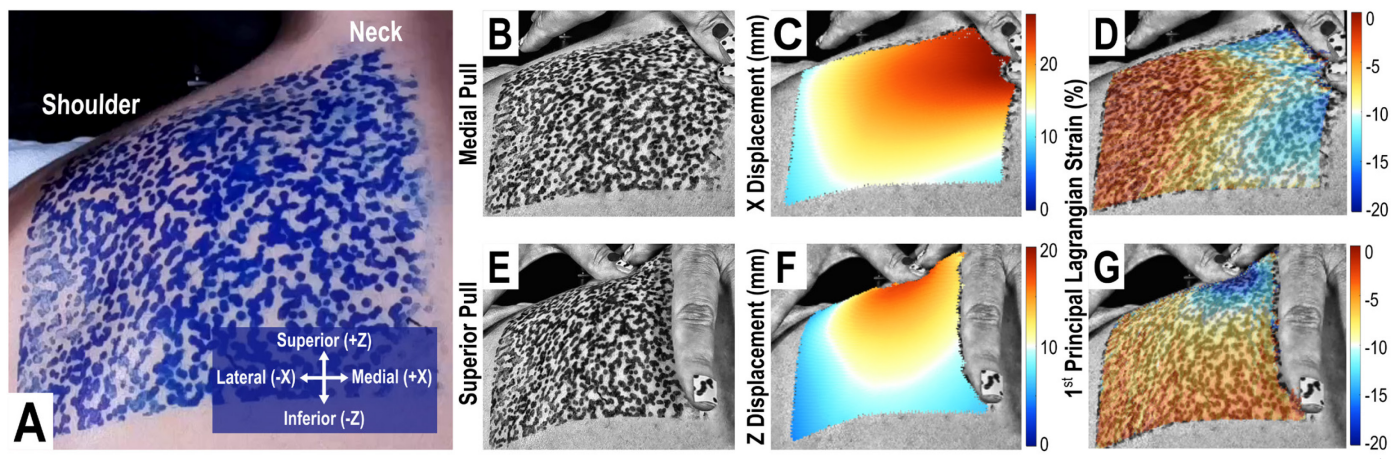


Fig. 2. Skin surface tracking of an ink speckle pattern with digital image correlation. (A) Raw image from one camera showing the ink speckle pattern (area ~100 cm²) applied at the left trapezius. The speckle size, density, and randomness inform the accuracy of the tracking and resolution of the resultant 3D point cloud. (B) Grayscale raw image showing pull in the medial direction applied manually by clinician's fingers. (C) 3D point cloud showing the change in skin surface displacement from the initial state ($t = 0 \rightarrow t = 2.7$ s). Red color depicts greater isolated movement, including rigid body motion, in the medial direction (+X) as compared to blue color, depicting minimal movement further away from manual contact. (D) Colormap overlayed on a raw image, showing the change in 1st principal Lagrangian strain ($t = 0 \rightarrow t = 2.7$ s). Red to blue color indicates increased compressive strain as compared to the resting state. (E-G) Raw image, isolated displacement, and 1st principal Lagrangian strain when manual pull is applied in the superior direction (+Z) (t = 15.7 s).

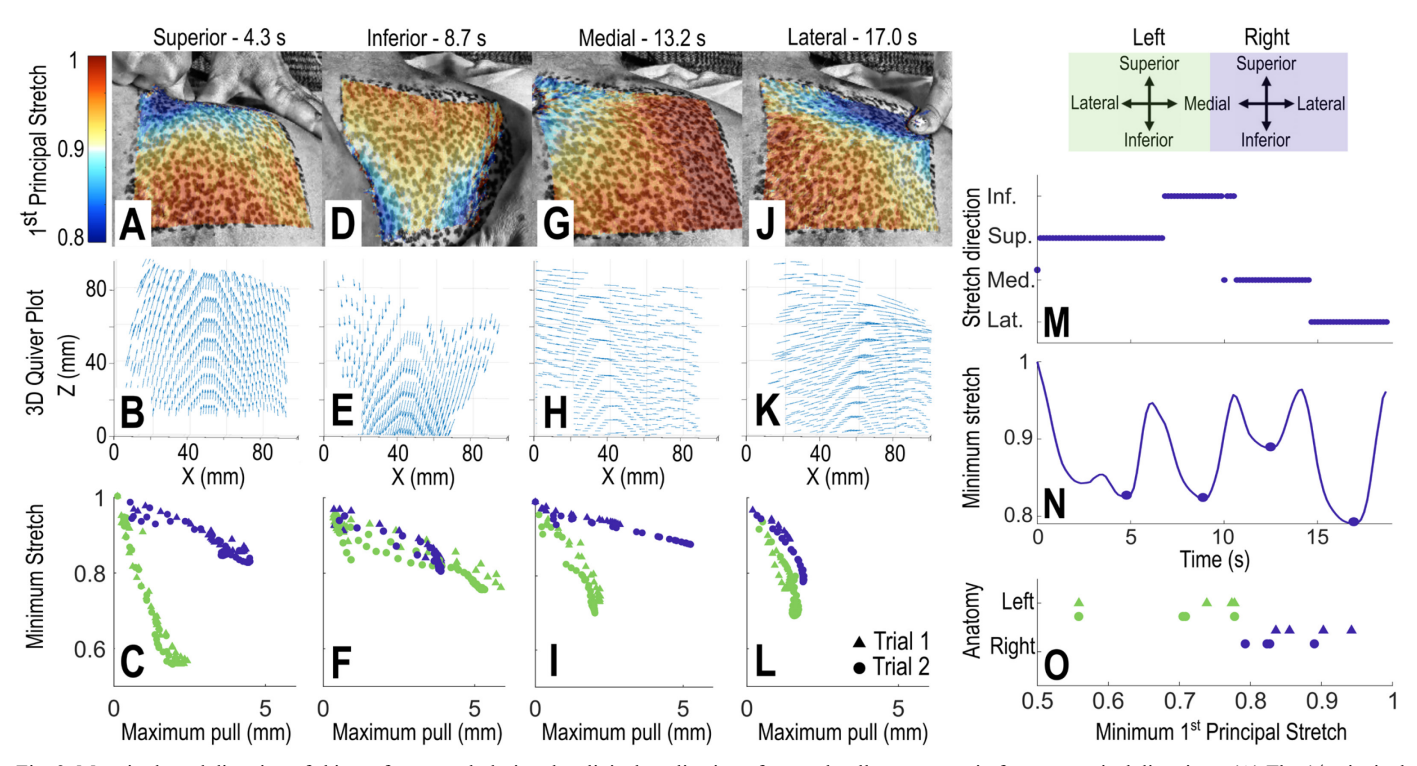


Fig. 3. Magnitude and direction of skin surface stretch during the clinical application of manual pull assessment in four anatomical directions. (A) The 1st principal stretch is depicted by the colormap overlayed on the image from one camera for manual pull in the superior direction (towards neck, 4.3 sec from start). A 1st principal stretch value of 1 (red) depicts no skin surface stretch between tracked points from the initial state. In contrast, a value of 0.8 (blue) depicts 20% compression in the tracked points from their initial state. Greater minimum stretch (i.e., a lower scale value) is measured near clinician finger contact and in the direction perpendicular to the manual pull. (B) The corresponding 3D quiver plot depicts skin surface movement as 3D vectors from their initial state, including rigid body motion. (C) Minimum stretch plotted against maximum pull, without rigid body motion. Clear separation between green (left) and purple (right) points indicates that at the same magnitude of manual pull, more compressive stretch is observed on the left side of the body. (D-L) Minimum 1st principal stretch, 3D quiver plots, and stretch-to-pull ratio in inferior, medial, and lateral directions. (M) From the 3D quiver plots, the pull direction can be categorized by isolating skin movement into 4 directions (-X, +X, -Z, +Z), and comparing maximum displacement. (N) The minima of the 1st principal stretch values in panels A, D, G, and J were measured at each image frame over the time duration of the clinical assessment. The four distinct valleys align with the four pull directions in panel M. (O) The minimum 1st principal stretch values from panel N, and for all 4 pull experiments for this participant (trial 1 – left and right, trial 2 – left and right, trial 1 – left and right, trial 2 – left and right, seem to the participant's left side may reflect differences in the stiffness of underlying muscle, in this case, that the

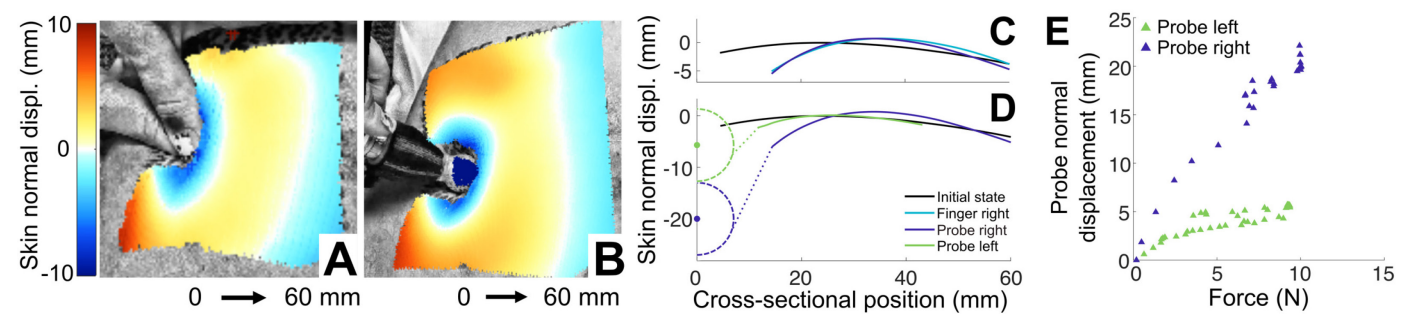


Fig. 4. Manual and instrumented force probe compression techniques generate similar patterns of skin surface deformation, and bilateral distinctions. (A) Normal displacement of the skin surface in response to manual compression by clinician on the right trapezius. Skin near the point of contact moves downward into the body as depicted by the blue color. (B) Similar data for instrumented force probe compression for the same clinician, participant, and body side. (C) Cross-sections of 3D normal displacement taken before contact (black) and at maximum indentation for finger (blue) and instrumented force probe (purple) compression on the right side of the body, where the latter two highly overlap, indicating the probe well mimics manual compression. (D) Cross-sectional comparison of instrumented force probe compression on right (purple) and left (green) sides of the body (trial 1), indicating a bilateral distinction. The solid lines depict surface points tracked with DIC while the dotted lines depict a projected connection between the imaged skin surface and tracked probe. (E) Plots of the instrumented force probe tip's normal displacement and recorded force (left and right sides of the body) show a steeper increase in probe normal displacement at a lower force on the right side, suggesting less stiff myofascial tissue on the right side as compared to the left, in agreement with the bilateral distinctions in the cross-sectional images in panel D.

components with the largest vector informing the direction of pull, i.e., +Z (superior), -Z (inferior), +X (lateral or medial, depending on side of body), and -X (medial or lateral) (Fig. 3B, E, H, K). Second, we determine the minimum stretch. The 1st principal stretch quantifies the change in distance between tracked pixels of a 3D point cloud (Fig. 3A, D, G, J). A stretch value of 0.8 depicts a 20% compression between tracked points, while a value of 1 depicts no change. A lower stretch value, or larger compression, is observed near the point of manual pull. The compression in tracked points is more readily observable in the 3D quiver plots (Fig. 3B, E, H, K) with vectors near the point of contact closer together than those further away. Upon classifying the pull direction (Fig. 3M), the minimum 1st principal stretch values are plotted at each time point (Fig. 3N) and align with each pull direction. Moreover, in Fig. 3O, a significant difference (t(7) = -3.98, p < 0.005) is found between the minimum stretch of the left and right sides for this participant.

Third, we quantify the skin mobility biomarker as the relationship between minimum stretch and maximum pull. As the magnitude of pull performed by the clinician was not monitored quantitatively, but left to clinical judgment, we calculate the maximum skin displacement in each direction after the homogenous displacement, or rigid body motion, is removed. Maximum pull for a given direction is measured as the 95th percentile of the isolated deformation data, following convention to avoid noise [39]. The minimum stretch value (Fig. 3N) is then plotted against the maximum pull value at each time point (Fig. 3C, F, I, L). For this participant, the superior and medial manual pull directions lead to clear distinctions bilaterally, but not with manual pull in the inferior direction.

B. Baseline tissue stiffness measure

To develop a baseline characterization for tissue stiffness, we develop force-displacement relations from the instrumented force probe and camera/DIC quantification of displacement. With these measurements, first, we compare manual and probebased compression. In Fig. 4A-B, the normal displacement of the skin surface is plotted for both cases for one participant. Similar fields of normal displacement are observed, with a minimum normal displacement of 9.47 mm for manual

compression and 9.83 mm for probe compression. Further, cross-sections of normal displacement at maximum indentation from manual (blue) and probe (purple) compression highly overlap (Fig. 4C). These findings indicate that probe indentation reasonably mimics manual compression. Second, we evaluate the tracking of the force probe's tip via the DIC cameras. In Fig. 4D, 2D cross-sections of surface deformation during probe compression are compared between the participant's left and right sides. A bilateral distinction is evident. Also, the clinician reaches an indentation depth of 19.98 mm on the right side, presumably related to the participant's pain threshold, and in contrast only a depth of 5.69 mm on the left side.

Third, in Fig. 4E, we develop the force-displacement relationship. While maximum force levels are similar bilaterally (right: 9.93 N, left: 9.34 N), despite the clinician not being given feedback on their employed force, displacement varies significantly. As this plot indicates, at similar levels of force, displacement levels are much higher on the right side of the body than on the left, indicating the left side offers greater resistance to compression and is stiffer.

C. Differentiating bilateral stiffness with both approaches

We bilaterally compare the results between the skin mobility biomarker, and force-displacement measurements, across the four participants (Fig. 5). First, for the skin mobility biomarker and manual pull in the superior direction, we observe clear bilateral separation (Fig. 5A). In specific, at a maximum pull of ~2 mm, the minimum stretch is 0.56 on the left side of the body, indicating that the skin is compressing to a maximum of 44% at the point of peak manual pull. However, on the right side, at similar pull levels, the minimum stretch is only 0.93, or a maximum compression of 7%. Similar left and right distinctions are observed for participants in Figs. 5C and G, with the former participant exhibiting higher ratios of skin compression to pull on the right side of the body. In contrast, the participant in Fig. 5E does not exhibit a bilateral distinction.

Second, in these studies neither the force nor displacement magnitude of pull was monitored quantitatively, but left to clinical judgment. As such, when considering the magnitude of force, higher normal displacement of the probe indicates less material resistance to deformation, or lower stiffness (Fig. 5B).

At a force of ~13.5 N, the probe depth is greater on the right side of the body as compared to the left side (20.82 mm, 5.07 mm), indicating higher tissue stiffness on this participant's left side. Similar trends are observed for participants in Fig. 5D and H with the former exhibiting greater tissue stiffness on the right side of the body. In contrast, the participant in Fig. 5F does not exhibit a distinction bilaterally.

Third, and finally, to compare the efficacy of the skin mobility biomarker in bilaterally differentiating a participant's tissue stiffness, we compare its results to that of the stiffness metric obtained using the probe. Matching the rows in Fig. 5, clear bilateral distinctions are observable, and in the same directions, for three of the four participants, with the last participant in Fig. 5E and F not exhibiting a bilateral distinction.

V. DISCUSSION

This work develops mechanical biomarkers based upon observations of skin surface deformation, captured with digital image correlation, and evaluates their ability to infer myofascial differences in bilateral anatomy during soft tissue manipulation. The agreement of the skin mobility biomarker and forcedisplacement measurements in this case study suggests that the deformation of the skin surface can provide inference into underlying myofascial stiffness. The development of a skin surface biomarker able to differentiate stiffness differences felt by a clinician may enable greater precision in affective touch therapies used to assess and treat myofascial pain. Additionally, these biomarkers can inform design requirements for innovations in medical haptics such as clinical training simulations, tele-remote assessment and treatment, and knot detection via robotic massage. Moreover, the biomarkers described herein do not impede direct skin contact between clinicians and their patients.

Across both metrics, derived from the skin surface alone or force load, the results depict clear bilateral differences (Fig. 5A-D, G, H). Furthermore, the body side measuring greater skin surface compression aligns with higher force-displacement (stiffness) magnitudes, preliminarily suggesting a relationship between skin mobility during STM manual pull and underlying myofascial stiffness. We hypothesize that as musculoskeletal regions increase in stiffness, the underlying tissue becomes less responsive to movement, both normally and laterally, requiring that the skin must compress more to accommodate manually imposed displacement. As such, an increase in skin compression during manual pull may be a useful predictor in assessing myofascial mobility. Future experiments will include an increase in participants and trials to allow for statistical analysis of biomarker differentiation.

While the preliminary results of this case study show the approach's promise, further studies are needed to examine the efficacy of derived skin surface biomarkers in robustly differentiating and classifying myofascial pain states, including normal, latent, and active [40], as well as quantifying the direct effects of treatment on pain and mobility. In this regard, the work herein did not examine the effect of treatment, except for a very minor one-minute hold on the muscle. Moreover, biomarker measurements over time might provide insight into patient-specific treatment plans, including optimal treatment duration. To do this, methods need to be developed to track skin regions over long periods of time, and as well, perhaps that does not

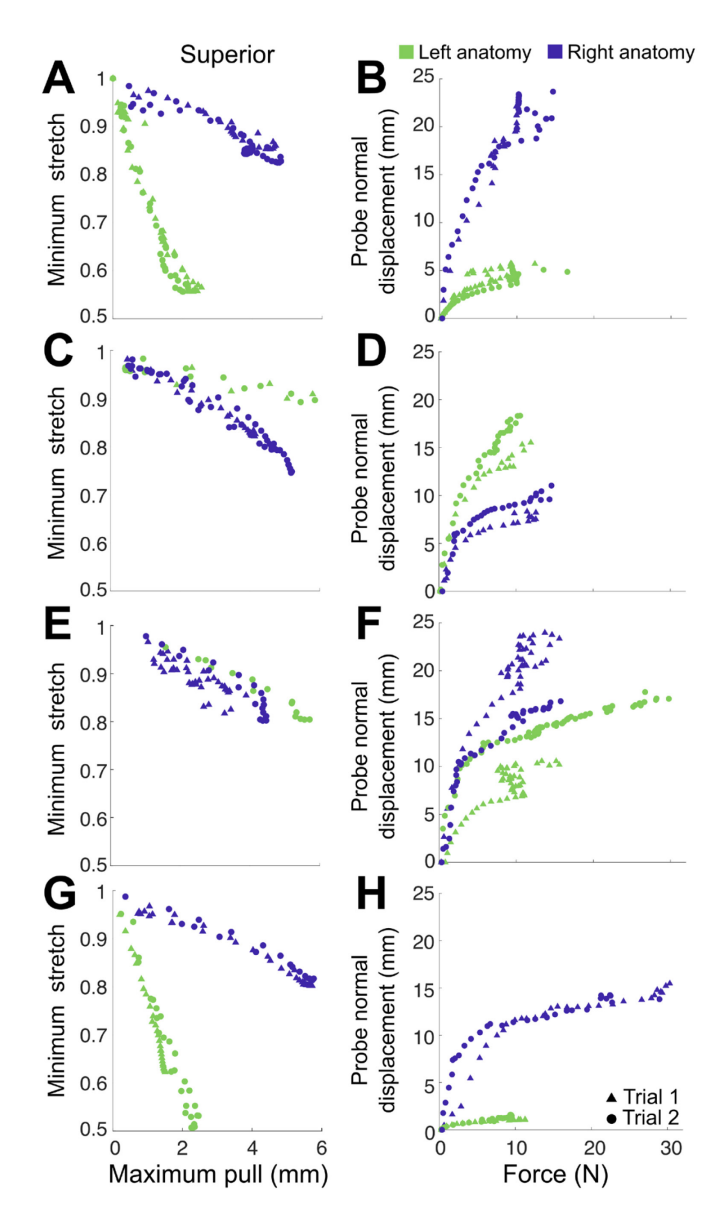


Fig. 5. A comparison of two developed mechanical biomarkers to assess bilateral stiffness based on 1) skin surface stretch upon manual pull with the clinician's fingers and 2) probe force and displacement, for the four participants. (A) Minimum stretch against maximum pull, in the superior pull direction, for the participant from Figs. 3 and 4. Clear separation is observed between points in green (left side) and purple (right side) across trials 1 (triangle) and 2 (circle), suggesting distinct skin surface movement differences bilaterally. (B) For the same participant, measured force during instrumented (probe) compression against normal displacement also suggests distinct differences in myofascial stiffness bilaterally. (C-H) The same quantities are repeated for the other three participants. The data for participants 1, 2, and 4 (rows A, C, and G) indicate that increases in the stiffness mechanical biomarker, as compared bilaterally, agree with the skin mobility biomarker. This finding likely indicates that when myofascial mobility is lower, musculoskeletal regions may be more stiff and as such, the skin surface accounts for more of the mobility, seen as lower minimum stretch, or increased skin surface compression during manual pull.

require the application of ink to the skin. Overall, while these findings warrant further study in larger and more diverse clinical populations, the development of mechanical biomarkers could have sustainable impact on clinical practice, enabling evidence-based myofascial assessment and intervention to ameliorate the suffering of patients with myofascial origins of pain.

ACKNOWLEDGMENT

This work was supported in part by NSF grants IIS-1908115 and NRT-1829004 and NIH grants R01NS105241, R21AT011980, and U24AT011970.

REFERENCES

- [1] T. Sundberg, H. Cramer, D. Sibbritt, J. Adams, and R. Lauche, "Prevalence, patterns, and predictors of massage practitioner utilization: Results of a US nationally representative survey," *Musculoskelet. Sci. Pract.*, vol. 32, pp. 31–37, Dec. 2017, doi: 10.1016/j.msksp.2017.07.003.
- [2] M. F. Barbe et al., "Key indicators of repetitive overuse-induced neuromuscular inflammation and fibrosis are prevented by manual therapy in a rat model," BMC Musculoskelet. Disord., vol. 22, no. 1, p. 417, May 2021, doi: 10.1186/s12891-021-04270-0.
- [3] G. M. Bove et al., "Manual therapy prevents onset of nociceptor activity, sensorimotor dysfunction, and neural fibrosis induced by a volitional repetitive task," PAIN, vol. 160, no. 3, pp. 632–644, Mar. 2019, doi: 10.1097/j.pain.00000000001443.
- [4] C. Haas *et al.*, "Massage timing affects postexercise muscle recovery and inflammation in a rabbit model," *Med. Sci. Sports Exerc.*, vol. 45, no. 6, pp. 1105–1112, Jun. 2013, doi: 10.1249/MSS.0b013e31827fdf18.
- [5] M. Rapaport et al., "Acute swedish massage monotherapy successfully remediates symptoms of generalized anxiety disorder: a proof-of-concept, randomized controlled study," J. Clin. Psychiatry, vol. 77, pp. e883–e891, Jul. 2016, doi: 10.4088/JCP.15m10151.
- [6] "AMTA," American Massage Therapy Association. https://www.amtamassage.org/.
- [7] T. Loghmani M and S. Bane, "Instrument-assisted soft tissue manipulation: evidence for its emerging efficacy," *J. Nov. Physiother.*, vol. s3, 2016, doi: 10.4172/2165-7025.S3-012.
- [8] D. W. Van Pelt, M. M. Lawrence, B. F. Miller, T. A. Butterfield, and E. E. Dupont-Versteegden, "Massage as a mechanotherapy for skeletal muscle," *Exerc. Sport Sci. Rev.*, vol. 49, no. 2, pp. 107–114, Apr. 2021, doi: 10.1249/JES.0000000000000244...
- [9] A. Bhattacharjee, S. Y. P. Chien, S. Anwar, and M. T. Loghmani, "Quantifiable soft tissue manipulation (qstmtm) - a novel modality to improve clinical manual therapy with objective metrics," *Annu. Int. Conf. IEEE Eng. Med. Biol. Soc. IEEE Eng. Med. Biol. Soc. Annu. Int. Conf.*, vol. 2021, pp. 4961–4964, Nov. 2021, doi: 10.1109/EMBC46164.2021.9629616.
- [10] A. Bhattacharjee, S. Anwar, S. Chien, and M. T. Loghmani, "A handheld quantifiable soft tissue manipulation device for tracking real-time dispersive force-motion patterns to characterize manual therapy treatment," *IEEE Trans. Biomed. Eng.*, vol. PP, Nov. 2022, doi: 10.1109/TBME.2022.3222124.
- [11] C. H. Karels, W. Polling, S. M. A. Bierma-Zeinstra, A. Burdorf, A. P. Verhagen, and B. W. Koes, "Treatment of arm, neck, and/or shoulder complaints in physical therapy practice," *Spine*, vol. 31, no. 17, pp. E584-589, Aug. 2006, doi: 10.1097/01.brs.0000229229.54704.77.
- [12] S. W. Cheatham, R. Baker, and E. Kreiswirth, "Instrument assisted soft-tissue mobilization: A commentary on clinical practice guidelines for rehabilitation professionals," *Int. J. Sports Phys. Ther.*, vol. 14, no. 4, pp. 670–682, Jul. 2019.
- [13] C. B. Seffrin, N. M. Cattano, M. A. Reed, and A. M. Gardiner-Shires, "Instrument-assisted soft tissue mobilization: a systematic review and effect-size analysis," *J. Athl. Train.*, vol. 54, no. 7, pp. 808–821, Jul. 2019, doi: 10.4085/1062-6050-481-17.
- [14] G. M. Gehlsen, L. R. Ganion, and R. Helfst, "Fibroblast responses to variation in soft tissue mobilization pressure," *Med. Sci. Sports Exerc.*, vol. 31, no. 4, pp. 531–535, Apr. 1999, doi: 10.1097/00005768-199904000-00006.

- [15] C. J. Davidson, L. R. Ganion, G. M. Gehlsen, B. Verhoestra, J. E. Roepke, and T. L. Sevier, "Rat tendon morphologic and functional changes resulting from soft tissue mobilization," *Med. Sci. Sports Exerc.*, vol. 29, no. 3, pp. 313–319, Mar. 1997, doi: 10.1097/00005768-199703000-00005.
- [16] K. J. Sherman, A. J. Cook, J. R. Kahn, R. J. Hawkes, R. D. Wellman, and D. C. Cherkin, "Dosing study of massage for chronic neck pain: protocol for the dose response evaluation and analysis of massage [DREAM] trial," *BMC Complement. Altern. Med.*, vol. 12, p. 158, Sep. 2012, doi: 10.1186/1472-6882-12-158.
- [17] C. Haas, T. M. Best, Q. Wang, T. A. Butterfield, and Y. Zhao, "In vivo passive mechanical properties of skeletal muscle improve with massage-like loading following eccentric exercise," *J. Biomech.*, vol. 45, no. 15, pp. 2630–2636, Oct. 2012, doi: 10.1016/j.jbiomech.2012.08.008.
- [18] "American Physical Therapy Association," APTA. https://www.apta.org/.
- [19] S. Engell, J. J. Triano, J. R. Fox, H. M. Langevin, and E. E. Konofagou, "Differential displacement of soft tissue layers from manual therapy loading," *Clin. Biomech.*, vol. 33, pp. 66–72, Mar. 2016, doi: 10.1016/j.clinbiomech.2016.02.011.
- [20] J. Vappou, C. Maleke, and E. E. Konofagou, "Quantitative viscoelastic parameters measured by harmonic motion imaging," *Phys. Med. Biol.*, vol. 54, no. 11, pp. 3579–3594, Jun. 2009, doi: 10.1088/0031-9155/54/11/020.
- [21] S. C. Hauser, S. McIntyre, A. Israr, H. Olausson, and G. J. Gerling, "Uncovering human-to-human physical interactions that underlie emotional and affective touch communication," in 2019 IEEE World Haptics Conference (WHC), Jul. 2019, pp. 407–412. doi: 10.1109/WHC.2019.8816169.
- [22] S. C. Hauser, S. S. Nagi, S. McIntyre, A. Israr, H. Olausson, and G. J. Gerling, "From human-to-human touch to peripheral nerve responses," in 2019 IEEE World Haptics Conference (WHC), Jul. 2019, pp. 592–597. doi: 10.1109/WHC.2019.8816113.
- [23] C. Lo, S. T. Chu, T. B. Penney, and A. Schirmer, "3D hand-motion tracking and bottom-up classification sheds light on the physical properties of gentle stroking," *Neuroscience*, Sep. 2020, doi: 10.1016/j.neuroscience.2020.09.037.
- [24] I. Oikonomidis, N. Kyriazis, and A. Argyros, "Efficient model-based 3D tracking of hand articulations using Kinect," in *Proceedings of the British Machine Vision Conference 2011*, Dundee, 2011, p. 101.1-101.11. doi: 10.5244/C.25.101.
- [25] S. Sridhar, F. Mueller, A. Oulasvirta, and C. Theobalt, "Fast and robust hand tracking using detection-guided optimization," in 2015 IEEE Conference on Computer Vision and Pattern Recognition (CVPR), Jun. 2015, pp. 3213–3221. doi: 10.1109/CVPR.2015.7298941.
- [26] E. K. Vonstad, X. Su, B. Vereijken, K. Bach, and J. H. Nilsen, "Comparison of a deep learning-based pose estimation system to marker-based and Kinect systems in exergaming for balance training," *Sensors*, vol. 20, no. 23, Art. no. 23, Jan. 2020, doi: 10.3390/s20236940.
- [27] Y. Zhou, M. Habermann, W. Xu, I. Habibie, C. Theobalt, and F. Xu, "Monocular real-time hand shape and motion capture using multi-modal data," presented at the Proceedings of the IEEE/CVF Conference on Computer Vision and Pattern Recognition, 2020, pp. 5346–5355.
- [28] B. Li, S. Hauser, and G. J. Gerling, "Identifying 3-D spatiotemporal skin deformation cues evoked in interacting with compliant elastic surfaces," in 2020 IEEE Haptics Symposium (HAPTICS), Mar. 2020, pp. 35–40. doi: 10.1109/HAPTICS45997.2020.ras.HAP20.22.5a9b38d8.
- [29] S. C. Hauser and G. J. Gerling, "Imaging the 3-D deformation of the finger pad when interacting with compliant materials," in 2018 IEEE Haptics Symposium (HAPTICS), Mar. 2018, pp. 7– 13. doi: 10.1109/HAPTICS.2018.8357145.
- [30] A. R. Kao, C. Xu, and G. J. Gerling, "Using digital image correlation to quantify skin deformation with von frey

- monofilaments," *IEEE Trans. Haptics*, vol. 15, no. 1, pp. 26–31, Jan. 2022, doi: 10.1109/TOH.2021.3138350.
- [31] X. Liu, R. Maiti, Z. H. Lu, M. J. Carré, S. J. Matcher, and R. Lewis, "New non-invasive techniques to quantify skin surface strain and sub-surface layer deformation of finger-pad during sliding," *Biotribology*, vol. 12, pp. 52–58, Dec. 2017, doi: 10.1016/j.biotri.2017.07.001.
- [32] R. Maiti *et al.*, "In vivo measurement of skin surface strain and sub-surface layer deformation induced by natural tissue stretching," *J. Mech. Behav. Biomed. Mater.*, vol. 62, pp. 556–569, Sep. 2016, doi: 10.1016/j.jmbbm.2016.05.035.
- [33] X. Hu *et al.*, "Skin surface and sub-surface strain and deformation imaging using optical coherence tomography and digital image correlation," in *Optical Elastography and Tissue Biomechanics III*, Mar. 2016, vol. 9710, p. 971016. doi: 10.1117/12.2212361.
- [34] Z. S. Lee, R. Maiti, M. J. Carré, and R. Lewis, "Morphology of a human finger pad during sliding against a grooved plate: A pilot study," *Biotribology*, vol. 21, p. 100114, Mar. 2020, doi: 10.1016/j.biotri.2019.100114.
- [35] Z. Xu, J. D. Cruz, C. Fthenakis, and C. Saliou, "A novel method to measure skin mechanical properties with three-dimensional

- digital image correlation," *Skin Res. Technol.*, vol. 25, no. 1, pp. 60–67, 2019., doi: 10.1111/srt.12596.
- [36] D. Solav, K. M. Moerman, A. M. Jaeger, K. Genovese, and H. M. Herr, "MultiDIC: An open-source toolbox for multi-view 3d digital image correlation," *IEEE Access*, vol. 6, pp. 30520–30535, 2018, doi: 10.1109/ACCESS.2018.2843725.
- [37] J. Blaber, B. Adair, and A. Antoniou, "Ncorr: Open-source 2d digital image correlation matlab software," *Exp. Mech.*, vol. 55, no. 6, pp. 1105–1122, Jul. 2015, doi: 10.1007/s11340-015-0009-1
- [38] D. Morgan, "Principles of soft tissue treatment," *J. Man. Manip. Ther.*, vol. 2, no. 2, pp. 63–65, Jan. 1994., doi: 10.1179/jmt.1994.2.2.63.
- [39] O. Levano Blanch, D. Lunt, G. J. Baxter, and M. Jackson, "Deformation behaviour of a fast diffusion bond processed from dissimilar titanium alloy powders," *Metall. Mater. Trans. A*, vol. 52, no. 7, pp. 3064–3082, Jul. 2021, doi: 10.1007/s11661-021-06301-w..
- [40] S. Vulfsons and A. Minerbi, "The case for comorbid myofascial pain-A qualitative review," *Int. J. Environ. Res. Public. Health*, vol. 17, no. 14, p. E5188, Jul. 2020., doi: 10.3390/ijerph17145188.